# Variable Extended Depth of Field Imaging Using Freeform Optics

Sara Moein\* and Thomas J. Suleski

Dept. of Physics & Optical Science, University of North Carolina at Charlotte, Charlotte, NC, USA 28223; Center for Freeform Optics, University of North Carolina at Charlotte, Charlotte, NC, USA 28223

# **ABSTRACT**

Increasing depth of field in imaging systems can be beneficial, particularly for systems with high numerical apertures and short depth of field, such as microscopy. Extending depth of field has been previously demonstrated, for example, using non-rotationally symmetric (freeform) components such as cubic and logarithmic phase plates. Such fixed phase plates are generally designed for a specific optical system, so a different phase plate is required for each system. Methods that enable variable extended depth of field for multiple optical systems could provide benefits by reducing the number of required components and costs. In this paper, we explore the design of a single pair of transmissive freeform surfaces to enable extended depth of field for multiple lenses with different numerical apertures through relative translation of the freeform components. This work builds on the concept of an Alvarez lens, in which one pair of transmissive XY-polynomial freeform surfaces generates variable optical power through lateral relative shifts between the surfaces. The presented approach is based on the design of multiple fixed phase plates to optimize the through-focus Modulation Transfer Function (MTF) for imaging lenses of given numerical apertures. The freeform surface equation for the desired variable phase plate pair is then derived and the relative shift amounts between the freeform surfaces are calculated to enable extended depth of field for multiple imaging lenses with different numerical aperture values. Design approaches and simulation results will be discussed.

**Keywords:** Extended depth of field, freeform optics, phase plates

#### 1. INTRODUCTION

Depth of Field (DoF) in imaging systems is defined as a range over which the system can produce an in-focus image; and it is inversely proportional to the square of Numerical Aperture (NA) of the imaging system. Therefore, systems with higher NA have shallow DoF. This can be problematic for applications such as microscopy with high magnification. As a result, methods to extend DoF in imaging systems are of special interest.

Researchers have previously demonstrated Extended Depth of Field (EDoF) imaging for microscopy using, for example, liquid lenses [1], deformable mirrors [2], and through the addition of phase plates. Different types of phase plates enable EDoF, including cubic, logarithmic and binary phase modulated plates [3-6]. Such phase plates alter the Point-Spread Function (PSF) of the system and trade image quality for a more consistent PSF through an extended range of defocus. Computational methods are then used to retrieve an image with higher quality [4]. Figure 1 illustrates a sample comparison between the through-focus spot diagrams for a 0.25 NA aspheric lens with and without a cubic phase plate ( $\lambda$ =633nm). It is evident that addition of the fixed phase plate has increased the spot sizes while making them less sensitive to defocus.

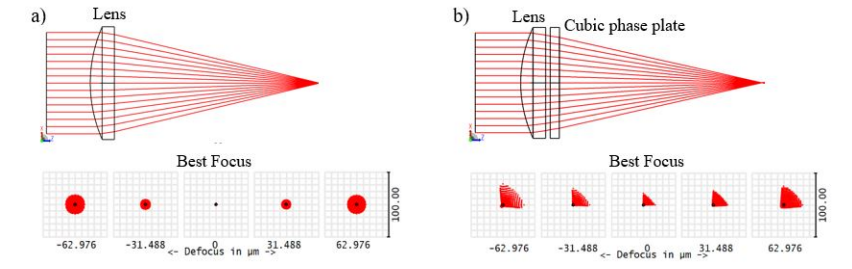


Figure 1. Through-focus spot diagrams for a 0.25 NA aspheric lens (a) without, and (b) with a cubic phase plate.

Optical systems with different NA's each need a custom fixed phase plate to extend DoF. Thus, methods that could enable variable EDoF for multiple imaging systems are desirable. In this paper, we discuss an approach that uses controlled movements between a pair of freeform phase plates to enable variable EDoF for different lenses. This is done by translating two XY freeform surfaces along the x-axis, which is demonstrated in Figure 2 below.

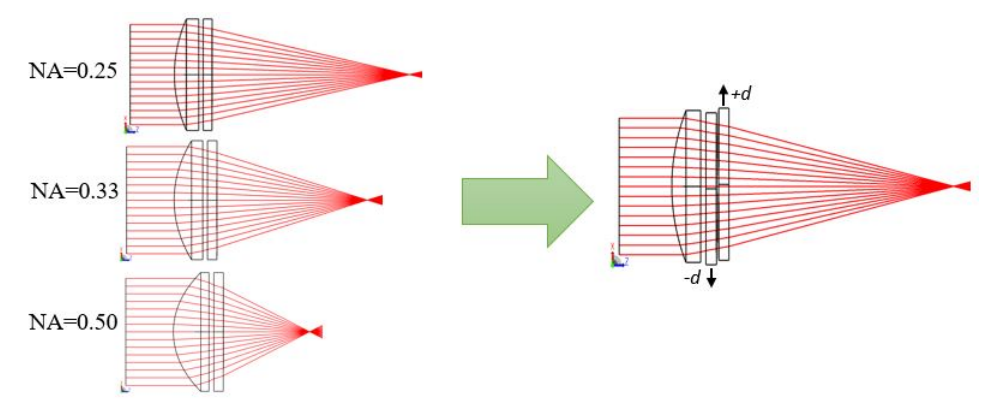


Figure 2. Replacing multiple fixed phase plates with one pair of freeforms that enables variable EDoF through relative translation of the freeform along x-axis.

The approach is similar to the concept of the Alvarez lens, which enables a variable focal length lens through relative translation of cubic freeform surfaces [7]. Hellmuth et al. [8] have previously shown a similar approach in which addition of a pair of phase plates at the exit pupil of an imaging system enables variable EDoF. This is achieved through relative translation of a phase plate pair with quartic surface equation,  $z(x,y)=\alpha(x^4+y^4)$ , along both the x- and y-axes in equal amounts and opposite directions in a manner analogous to work discussed by Lohmann for a varifocal lens [9]. Derivation of the surface equations and methods for obtaining the phase plate coefficients in [8] are not presented or discussed, but experimental results showed that the presented phase plate pair also introduces linear shifts in the image plane along both the x- and y-axes. Hellmuth et al. [8] also discussed the potential application of a shifted phase plate pair with a more complex surface equation (that also introduced a varifocal effect) in autofocus systems.

The approach we present in this paper enables variable EDoF imaging and introduces image displacement along only the x-axis. To find the proper surface equation for the phase plates, we follow a method discussed by Palusinski [10] that relates the surface equation of the phase plate pair and the composite effect of the shifted phase plates on the transmitted wavefront. We also present an MTF-based optimization method for the phase plate design.

# 2. DESIGN METHODOLOGY

# 2.1 Design approach

Dowski et al. [3] have shown that addition of a fixed cubic phase plate (CPP) at the pupil plane of an optical system extends the DoF for a nominal optical system. The surface equation of the CPP is given by:

$$Z(x,y) = \alpha(x^3 + y^3) \tag{1}$$

where the  $\alpha$  coefficient controls the phase amplitude. We build on this work and design multiple fixed CPP's, for imaging systems with a range of NAs. These CPP's are then replaced by a pair of transmissive freeform surfaces (Z<sub>t</sub>) that generates a variable cubic composite wavefront through relative translation of the phase components along the x-axis. Using the approach introduced by Palusinski et al. [10] the surface equation for the variable EDoF freeforms can be shown to be:

$$Z_f(x,y) = \beta \left(\frac{x^4}{4} + xy^3\right)$$

$$\beta = \frac{\alpha_{max}}{2d_{max}(n-1)}$$
(2)

$$\beta = \frac{\alpha_{max}}{2d_{max}(n-1)} \tag{3}$$

In Eqs. (2) and (3) above,  $\beta$  is calculated using the refractive index n of the phase plates, an  $\alpha_{max}$  coefficient that corresponds to the cubic coefficient for the highest NA lens, and the maximum desired shift between the freeform surfaces  $d_{max}$ . We refer to the elements described by Eq. (2) as a Quartic Phase Plate Pair (QPP). After calculating  $\beta$ , the shift amounts needed to enable EDoF for lower NA lenses can be found.

#### 2.2 Optical design and simulation

We first selected three commercial off-the-shelf aspheric lenses with NA values of 0.25, 0.33 and 0.5. The operating wavelength was set to 633 nm, and all phase plates were assumed to be fabricated from Polymethyl Methacrylate (PMMA) with 3 mm thicknesses. Designs and optimizations were performed in Zemax OpticStudio<sup>TM</sup>. The  $\alpha$  coefficient values were optimized for each lens through-focus. To define the through-focus range, we used half of the DoF as a baseline for each lens [11]:

$$DoF/2 = \Delta z = \frac{n\lambda}{NA^2} \tag{4}$$

where n is the refractive index of the surrounding medium,  $\lambda$  is the operating wavelength (633 nm) and NA is the numerical aperture of the aspheric lens. The cubic coefficient was optimized for image planes located at multiple integers of  $\Delta z$  (from  $-6\Delta z$  to  $+6\Delta z$ ). The optimization was performed by maximizing the through-focus MTF for each system at specific spatial frequencies and minimizing the differences between through-focus MTF values at selected frequencies.

This method improves the overall system performance while maintaining system MTF with less variance through-focus. After optimization of the  $\alpha$  coefficient for each system, the  $\beta$  coefficient was calculated based on EDoF requirements for the 0.5 NA lens. The relative shifts needed for the lower NA lenses were then calculated. The CPP surface and resulting QPP surface for a 0.25 NA lens are shown in Figure 3.

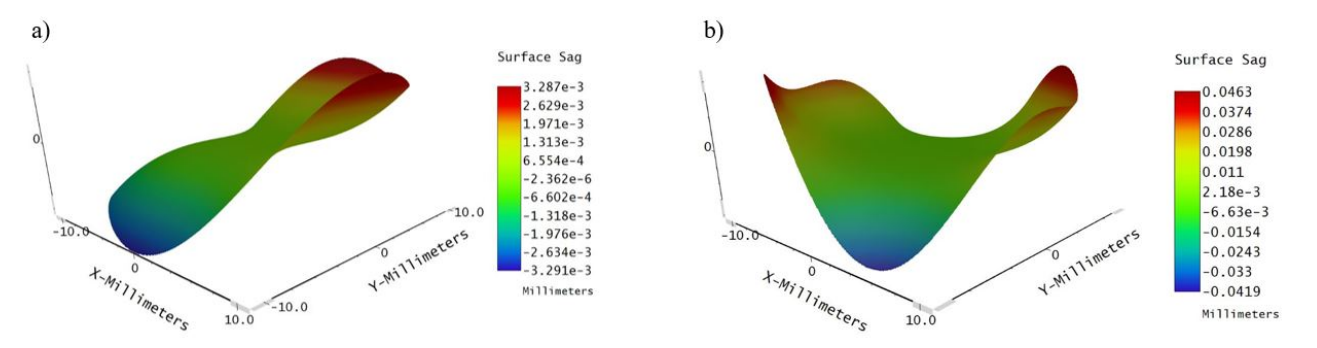


Figure 3. (a) Surface of designed CPP with  $\alpha = 2.473 \times 10^{-6}$  for 0.25 NA asphere, and (b) QPP surface with  $\beta = 9.205 \times 10^{-6}$ .

### 3. DESIGN RESULTS

## 3.1 Fixed phase plate (CPP) designs

Here, we report on results for design of three fixed cubic phase plates for three aspheric lenses with different NAs. Figure 4 includes through-focus spot diagrams ( $-6\Delta z$  to  $+6\Delta z$ ) for the selected lenses paired with the appropriate CPP. As expected, the spots become larger but are less sensitive to defocus with the addition of the CPP's.

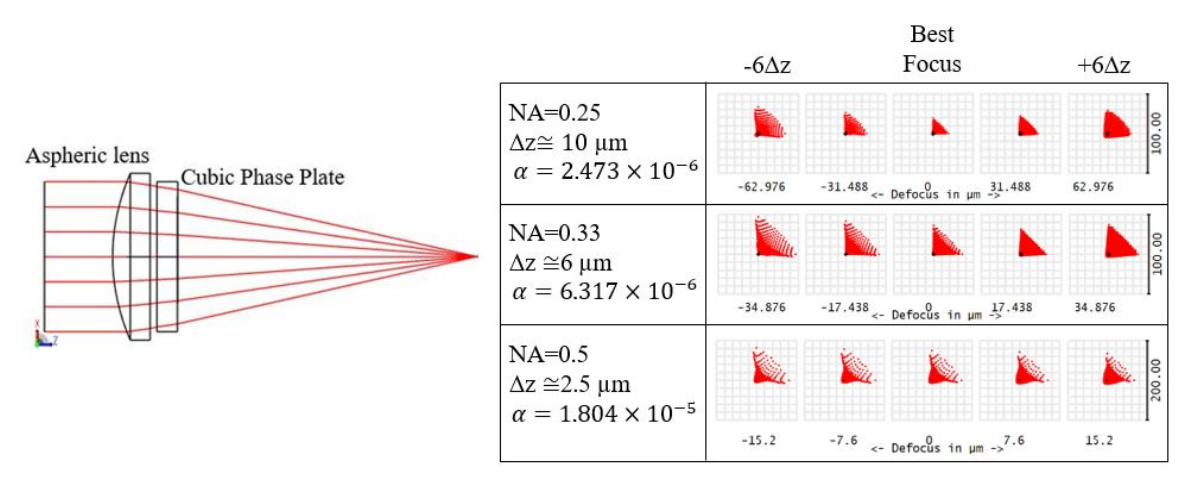


Figure 4. Through-focus spot diagrams for three aspheric lenses with fixed cubic phase plates.

### 3.2 Variable phase plate pair (QPP) design

One pair of variable phase plates was designed to enable variable EDoF through relative translation of the phase plates along the x-axis. Figure 5 demonstrates through-focus spot diagrams ( $-6\Delta z$  to  $+6\Delta z$ ) for the selected aspheric lenses with QPP ( $\beta=9.205\times10^{-6}$ ). The relative shift amounts are different for each lens based on their NA. The spot diagrams show that the spots with QPP are larger compared to the same lens systems with corresponding CPP, but are still less sensitive to defocus.

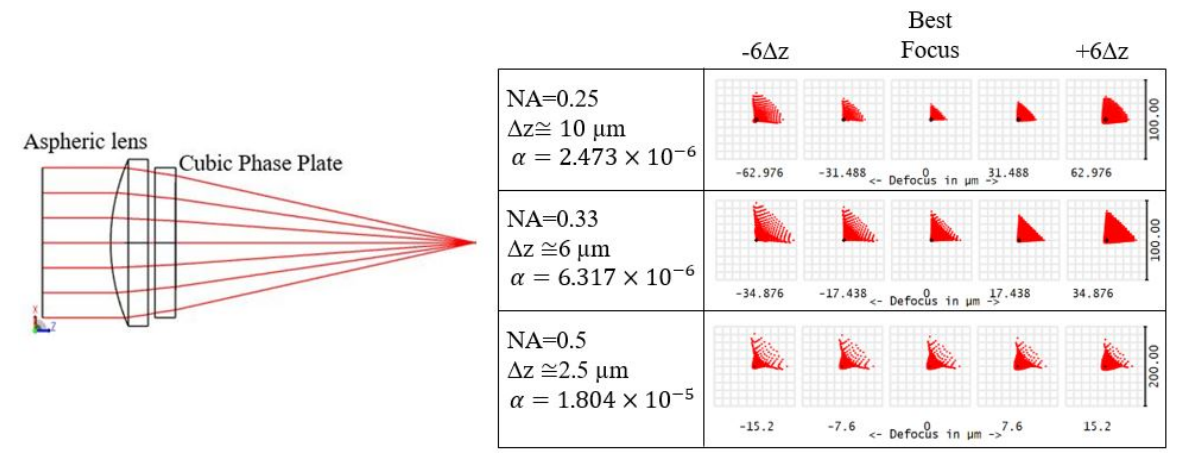


Figure 5. Through-focus spot diagrams for three aspheric lenses with variable EDoF phase plate pair (QPP).

## 4. PERFORMANCE COMPARISON

# 4.1 On-axis through-focus MTF

As mentioned previously, the optimization method presented here is an MTF-based approach with two main goals: (1) improving overall system performance, and (2) achieving more consistent through-focus performance. Figure 6 shows a comparison of on-axis through-focus MTF plots at three image planes ( $-4\Delta z$ , best focus and  $+4\Delta z$ ) for a 0.25 NA aspheric lens with and without the EDoF phase plates. These comparisons show that even though the aspheric lens has a near diffraction-limited performance at best focus, its performance degrades rapidly with defocus as expected. Qualitative examination of the MTF plots show that addition of the fixed (CPP) and variable phase plates (QPP) result in less MTF variation through-focus, but the overall performance of the systems are degraded relative to the performance of the aspheric lens at best focus, as expected.

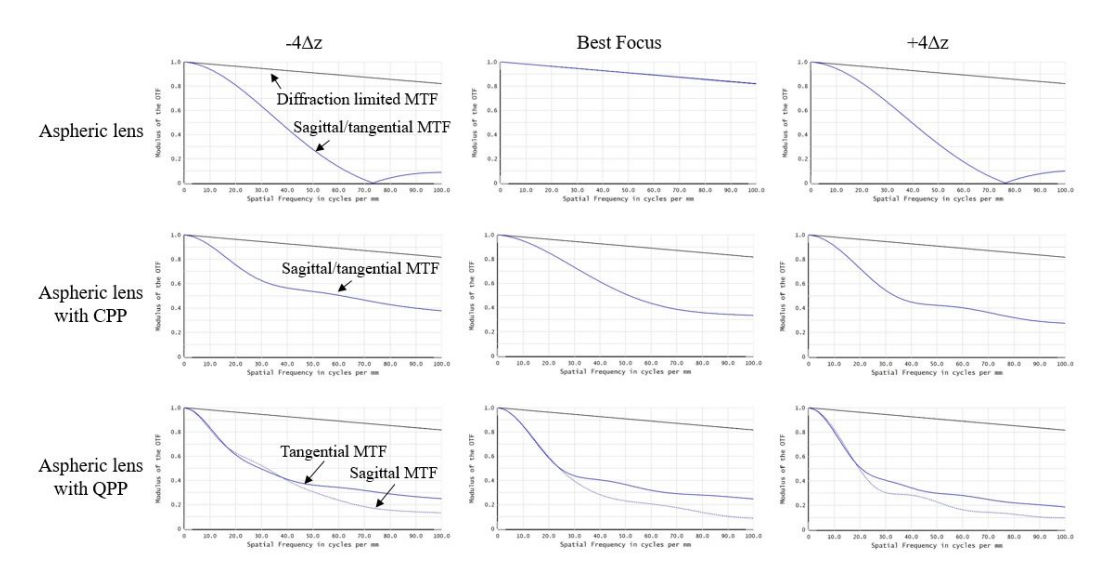


Figure 6. Through focus MTF plots  $(-4\Delta z \text{ to } +4\Delta z)$  for 0.25 NA aspheric lens without and with freeform phase plates.

## 4.2 On-axis Root-Mean-Square (RMS) deviation of PSF

The Point Spread Function (PSF) of a simple lens system varies throughout the range of defocus. Reduced through-focus variation in the PSF is expected with the addition of both the fixed and variable phase plates. Here, we suggest the RMS deviation of PSF (normalized to unity) as a quantitative measure to study through-focus variation of the systems. First, the Mean-Square-Error (MSE) between the PSF's at best focus and defocus image planes is calculated (point by point):

$$MSE = \frac{1}{m^2} \sum_{i=1}^{m} \sum_{j=1}^{m} \left( PSF_{d,i,j} - PSF_{f,i,j} \right)^2$$
 (5)

where  $m^2$  is the total number of samples in the PSF matrix and  $PSF_{d,i,j}$  and  $PSF_{f,i,j}$  represent the normalized PSF (in matrix form) at defocus and best focus image planes, respectively. Then, the RMS is found as:

$$RMS = \sqrt{MSE} \tag{6}$$

The RMS deviation of the normalized PSF is then plotted versus the defocus range of interest to compare the through-focus variation of the PSF for the different systems. Figure 7 demonstrates that use of the EDoF phase plates with the 0.25 NA aspheric lens results in smaller RMS deviations through-focus. These results also show that the proposed variable EDoF phase plates are comparable in performance to the multiple, fixed cubic phase plates.

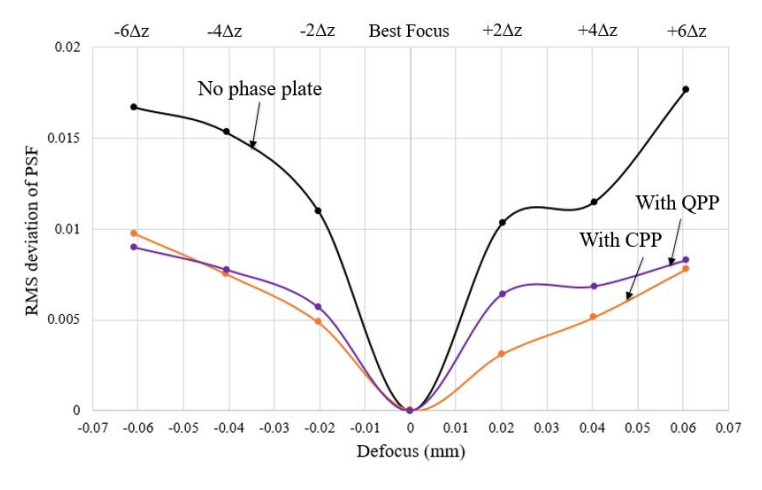


Figure 7. Comparison of RMS PSF deviation for 0.25 NA lens with and without fixed and variable EDoF phase plates.

## 4.3 Off-axis system performance

The presented design approach assumes on-axis illumination. Since off-axis performance of lens systems is important in imaging applications, we have also considered the performance of the phase plates over a range of field angles. Figure 8 shows through-focus spot diagrams for a 0.25 NA aspheric lens with CPP and QPP over a range of field angles along the y-axis. This comparison shows that as field angle increases, spot sizes become larger and more sensitive to defocus. Figure 9 demonstrates that at higher field angles, MTF at best focus worsens for both systems with CPP and QPP. Since EDoF phase plates are intended for imaging systems, design and optimization methods that include off-axis illumination are under development.

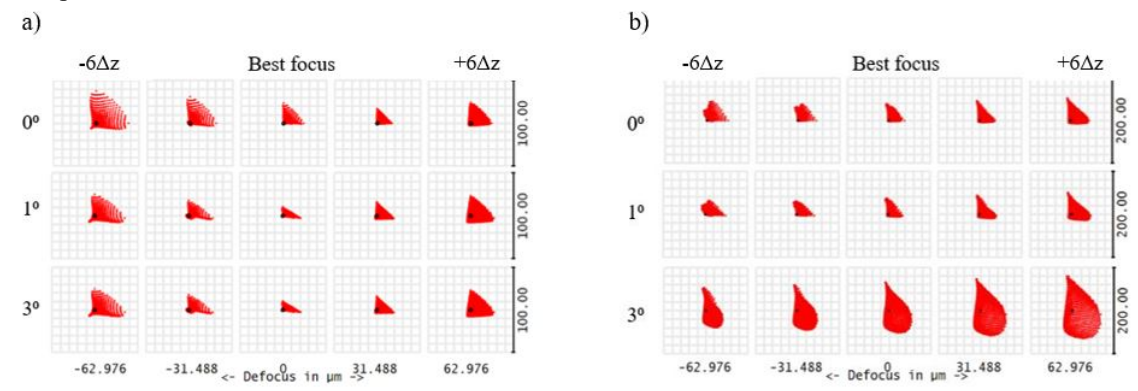


Figure 8. Through-focus spot diagrams for 0.25 NA aspheric lens with CPP (a) and QPP (b).

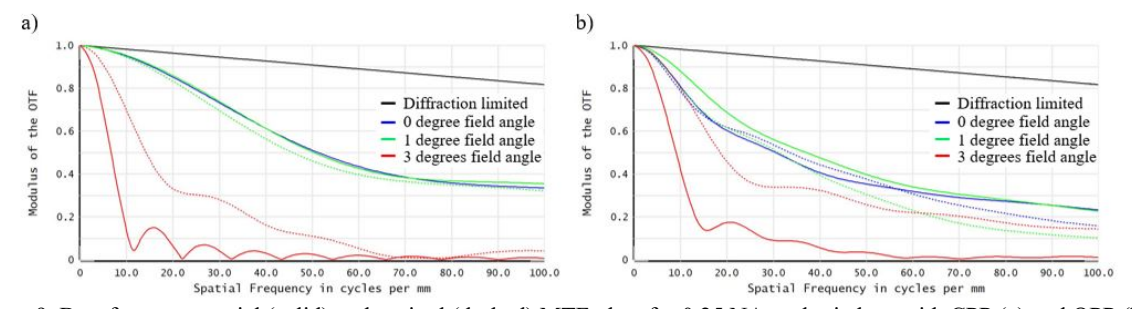


Figure 9. Best focus tangential (solid) and sagittal (dashed) MTF plots for 0.25 NA aspheric lens with CPP (a) and QPP (b).

#### 5. SUMMARY AND CONCLUSIONS

In conclusion, we designed one pair of transmissive freeforms that replaces multiple fixed EDoF phase plates to enable variable EDoF through relative translation of the freeform surfaces along the x-axis. The approach presented here enables variable EDoF for multiple imaging systems and could potentially reduce the cost for EDoF systems by reducing the number of required components. The optimization method discussed in this paper is based on MTF and targets improving overall system performance while achieving more consistent through-focus performance. Additionally, we have shown on-axis and off-axis performance of both fixed phase plates and variable phase plate pairs. The comparison demonstrates that these phase plates are sensitive to the addition of field angles. Additional work is underway on experimental fabrication and characterization, and design refinements for EDoF phase plates to maintain performance over a range of field angles and enable EDoF for higher NA imaging systems.

## 6. ACKNOWLEDGEMENTS

The authors would like to acknowledge useful discussions with Dr. Christoph Menke from Carl Zeiss AG, Dr. Sébastien Héron from THALES, and Dr. Jannick Rolland from the University of Rochester. This work was funded under the NSF I/UCRC Center for Freeform Optics (IIP-1822049 and IIP-1822026).

#### REFERENCES

- [1] Liu, S. and Hua, H., "Extended depth-of-field microscopic imaging with a variable focus microscope objective," Opt. Express 19, 353-362 (2011).
- [2] Shain, W., Vickers, N., Goldberg, B., Bifano, T., and Mertz, J., "Extended depth-of-field microscopy with a high-speed deformable mirror," Opt. Lett. 42, 995-998 (2017).
- [3] Dowski, E. R. and Cathey, W. T., "Extended depth of field through wave-front coding," Appl. Opt. 34, 1859-1866 (1995).
- [4] Tucker, S. C., Cathey, W. T., Cathey and Dowski, E. R., "Extended depth of field and aberration control for inexpensive digital microscope systems," Opt. Express 4, 467-474 (1999).
- [5] Sherif, S. S., Cathey, W. T. and Dowski, E. R., "Phase plate to extend depth of field of incoherent hybrid imaging systems," Appl. Opt. 43,2709-2721 (2004).
- [6] Wang, H., Shi, L., Yuan, G., Miao, X. S., Tan, W., and Chong, T., "Subwavelength and superresolution nondiffraction beam," Appl. Phys. Lett. 89, 171102 (2006).
- [7] Alvarez, L., W., "Two-element variable-power spherical lens," U.S Patent 3,305,294 (1967).
- [8] Hellmuth, T., Bich, A., Börret, R., Holschbach, A., and Kelm, A., "Variable phaseplates for focus invariant optical systems," Proc. SPIE 5962, Optical Design and Engineering II, 596215 (2005).
- [9] Lohmann, A. W., "A new class of varifocal lenses," Appl. Opt. 9(7), 1669 -1671 (1970).
- [10] Palusinski, I., A., Sasián, J., M., and Greivenkamp, J., E., "Lateral-shift variable aberration generators," Appl. Opt. 38, 86-90 (1999).
- [11] Tkaczyk, T. S., [Field Guide to Microscopy], SPIE, 9780819472465 (2010).